

COMPUTATION OF LAPLACIAN POTENTIALS BY AN EQUIVALENT-SOURCE METHOD

Prof. R. F. Harrington, Ph.D., K. Pontoppidan, Civ.Ing., P. Abrahamsen and N. C. Albertsen

An algorithm for the computation of the solution to Laplace's equation in a 2-dimensional region is given in terms of equivalent sources on the boundary. The region may be of an arbitrary shape, and the boundary conditions may be an arbitrary combination of Dirichlet, Neumann and impedance types. The solution is obtained by a moment method, using either a step approximation to the source, or a piecewise-linear approximation. Point matching is used for testing the boundary conditions. Computer programs are available for the general problem, and some electromagnetic-field applications are discussed.

List of symbols

- α, β, γ = arbitrary functions of c
- α_c = attenuation constant due to metallic losses
- $\eta = \sqrt{(\mu/\epsilon)}$ = intrinsic impedance of a medium
- σ = equivalent flux source on curve C
- ϵ = permittivity
- μ = permeability
- ρ = radius vector to a point (x, y)
- Φ = solution to Laplace's equation
- Ψ_i = potential from strip of uniform source on ΔC_i
- Δ_i = length of element ΔC_i of curve C
- c = length variable along curve C
- g = conductivity
- k = constant
- l_{ji} = elements of matrix $[l]$
- n = outward unit vector normal to curve C
- u = unit vector tangential to curve C
- w = complex function
- x, y = co-ordinates of point in space
- $z = x + jy$ = complex variable
- C = capacitance
- D = electric-flux density
- E = electric-field intensity
- H = magnetic-field intensity
- I = current
- J = current density
- P = power
- P_i = pulse function
- Q = electric charge
- R = resistance
- V = constant potential
- Z_0 = characteristic impedance of a transmission line
- * denotes a complex conjugate

1 Statement of problem

Laplace's equation is one of the most important differential equations of physics. In this paper, we give a convenient method for computing solutions to Laplace's equation in a region which is subject to general boundary conditions on the bounding surface. Only 2-dimensional problems are considered explicitly, but the procedure is applicable to Laplace's equation in three or more dimensions. The general method of solution is to transform the boundary-value problem into an integral equation,¹ and then to solve this integral equation by a moment method.^{2,3}

Consider a 2-dimensional region R bounded by the contour

C as shown in Fig. 1. Let the radius vector ρ denote the coordinates (x, y) of a point in space, the unit vector n denote the outward unit normal to C , and the variable c denote the

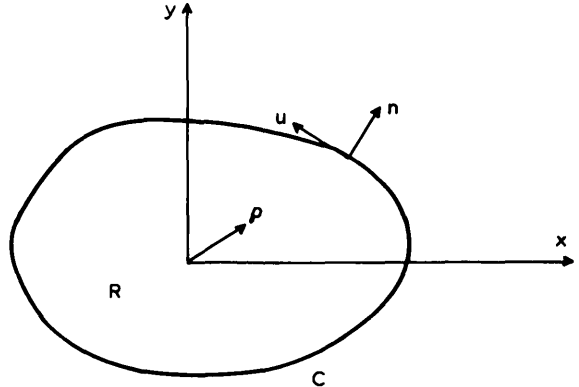


Fig. 1
Geometry of problem

length measured along C . The problem is to find $\Phi(\rho)$ in R which satisfies Laplace's equation

$$\frac{\partial^2 \Phi}{\partial x^2} + \frac{\partial^2 \Phi}{\partial y^2} = 0 \quad \dots \dots \dots (1)$$

in R , and the boundary condition

$$\alpha(c)\Phi + \beta(c) \frac{\partial \Phi}{\partial n} = \gamma(c) \quad \dots \dots \dots (2)$$

on C . Here α, β and γ are given functions of c . The general conditions of eqn. 2 include, as specialisations, the following cases:

- (a) Dirichlet boundary conditions, with Φ specified on C ($\alpha = 1, \beta = 0$)
- (b) Neumann boundary conditions, with $\partial\Phi/\partial n$ specified on C ($\alpha = 0, \beta = 1$)
- (c) impedance boundary conditions, with $\Phi/(\partial\Phi/\partial n)$ specified on C ($\alpha = 1, \gamma = 0$).

Also included are mixed boundary conditions, i.e. combinations of a, b and c over mutually exclusive subsections of C . In cases b and c it is necessary to specify Φ at one point in R or on C ; otherwise Φ is indeterminate by a constant.

2 Method of solution

An arbitrary Laplacian potential Φ in R can be produced by sources on C . If flux sources and dipole sources are allowed, there are infinitely many distributions on C which produce the same Φ in R . This concept, known as the equivalence principle,⁴ is discussed in terms of Green's theorem in Appendix 8.1. Letting $\sigma(c)$ denote a distribution of flux sources on C , the potential at any point ρ can be expressed by the superposition

$$\Phi(\rho) = \oint_C \sigma(c') \ln \frac{k}{|\rho - \rho'|} dc' \quad \dots \dots \dots (3)$$

Here k is a constant which, for reasons discussed in Section 4, is chosen so that

$$k > |\rho - \rho'|_{max} \quad \dots \dots \dots (4)$$

with ρ and ρ' on C . Specialising eqn. 3 to C , and applying the boundary condition of eqn. 2, we have

$$\left[\alpha\Phi + \beta \frac{\partial \Phi}{\partial n} \right]_{\rho \text{ on } C} = \gamma(c) \quad \dots \dots \dots (5)$$

Program CP 11, received 28th February 1969. The program listing and accompanying documentation are held in the IEE Program Library, IEE, Savoy Place, London WC2, England. Copies are available on application and payment of a handling charge. The authors are with the Laboratory of Electromagnetic Theory, Technical University of Denmark, Lyngby, Denmark. Prof. Harrington is on leave from the Department of Electrical Engineering, Syracuse University, Syracuse, NY, USA

This is an integral equation for determining σ on C . Once σ is found, Φ in R is given by eqn. 3. Eqn. 3 also applies externally to C , and we are solving the internal and external boundary-value problems simultaneously.

Approximate solutions to eqn. 5 can be obtained by the general method of moments.³ In this Section, we use pulse functions for expansion and point matching for testing. This gives a step approximation to the equivalent sources. In Appendix 8.2, the corresponding solution for a piecewise-linear approximation to σ is discussed.

Define N points ρ_i on C , $i = 1, 2, \dots, N$, and approximate C by the N straight-line segments ΔC_i between points i and $i + 1$. Consider the pulse functions

$$P_i(c) = \begin{cases} 1 & \text{on } \Delta C_i \\ 0 & \text{elsewhere} \end{cases} \quad (6)$$

and represent σ by the step approximation

$$\sigma \simeq \sum_{i=1}^N \sigma_i P_i(c) \quad (7)$$

Substituting eqn. 7 into eqn. 3, we obtain

$$\Phi(\rho) \simeq \sum_{i=1}^N \sigma_i \Psi_i(\rho) \quad (8)$$

$$\text{where } \Psi_i(\rho) = \int_{\Delta C_i} \frac{k}{|\rho - \rho'|} dc' \quad (9)$$

Now define points $\hat{\rho}_j$, $j = 1, 2, \dots, N$ as the midpoints of ΔC_j . Eqn. 8 is substituted into eqn. 5, and the resulting equation is satisfied at each ρ_j . This gives the set of equations

$$\sum_{i=1}^N \sigma_i l_{ji} = \gamma_j \quad j = 1, 2, \dots, N \quad (10)$$

where $\gamma_j = \gamma(\hat{\rho}_j)$ and

$$l_{ji} = \left[\alpha \Psi_i + \beta \frac{\partial \Psi_i}{\partial n} \right]_{\rho=\hat{\rho}_j} \quad (11)$$

Eqs. 10 can now be solved for σ_i , which gives a step approximation to σ according to eqn. 7.

This solution is conveniently expressed in matrix notation as follows. Let $[l]$ denote the square matrix of the l_{ji} , $[\sigma]$ the column matrix of the σ_i , and $[\gamma]$ the column matrix of the γ_i . Then eqns. 10 become

$$[l][\sigma] = [\gamma] \quad (12)$$

and the solution

$$[\sigma] = [l]^{-1}[\gamma] \quad (13)$$

Let $[P]$ denote the row matrix of the pulse functions P_i , defined by eqn. 6. Then the functional expression (eqn. 7) for the equivalent source is

$$\sigma = [P][\sigma] = [P][l]^{-1}[\gamma] \quad (14)$$

Finally, let $[\Psi]$ denote the row matrix of Ψ_i of eqn. 9. The potential Φ at any point ρ in R is then given by

$$\Phi = [\Psi][\sigma] = [\Psi][l]^{-1}[\gamma] \quad (15)$$

The matrix $[l]$ is usually well conditioned, and can be inverted by any convenient algorithm.

3 Evaluation of matrix elements

For the 2-dimensional case, the matrix elements can be conveniently evaluated using complex-function theory. Let $z = x + jy$ represent a point in space, and use the identities

$$\ln \frac{k}{|\rho - \rho'|} = \text{Re} \left(\ln \frac{k}{z - z'} \right) \quad (16)$$

$$dc' = |dz'| = dz'/u \quad (17)$$

where u is the unit tangent to C . Now eqn. 9 can be written as

$$\Psi_i = \text{Re}(w_i) \quad (18)$$

$$\text{where } w_i = \frac{1}{u_i} \int_{z_i}^{z_{i+1}} \ln \frac{k}{z - z'} dz' \quad (19)$$

Next, change variables according to $z - z' = kv$, and integrate $\ln v$ to obtain

$$w_i = \frac{k}{u_i} \left[v \ln v - v \right]_{(z-z_i)/k}^{(z-z_{i+1})/k} \quad (20)$$

This can be rearranged to

$$w_i(z) = \frac{z - z_i}{u_i} \ln \frac{z - z_{i+1}}{z - z_i} + \Delta_i \left(1 + \ln \frac{k}{z - z_{i+1}} \right) \quad (21)$$

$$\text{where } \Delta_i = |z_{i+1} - z_i| \quad (22)$$

$$u_i = (z_{i+1} - z_i)/\Delta_i \quad (23)$$

Ψ_i is given by the real part of eqn. 21, according to eqn. 18.

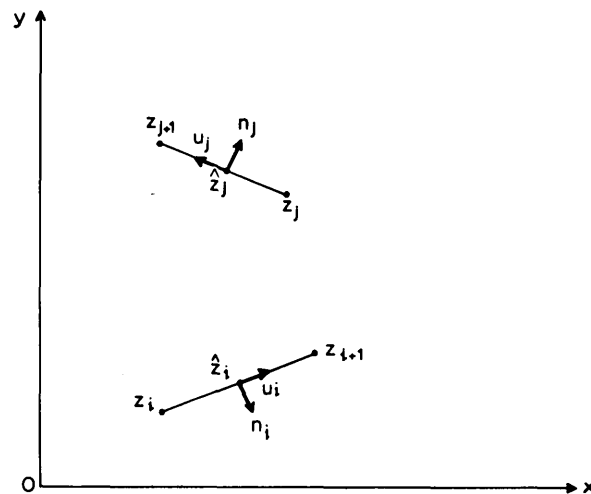


Fig. 2 Two segments ΔC_i and ΔC_j

Fig. 2 shows two straight-line segments ΔC_i and ΔC_j in the approximation of the contour C . The point

$$\hat{z}_j = (z_{j+1} + z_j)/2 \quad (24)$$

is the midpoint of ΔC_j , and the unit vectors n_j and u_j are normal and tangential to ΔC_j , respectively. To evaluate the matrix elements by eqn. 11, in addition to Ψ_i , we need $\partial \Psi_i / \partial n_j$. In terms of complex quantities⁵,

$$\Delta \Psi = \left(\frac{dw}{dz} \right)^* \quad (25)$$

$$a \cdot b = \text{Re}(ab^*) \quad (26)$$

Now $n_j = -ju_j$, whence

$$\begin{aligned} \frac{\partial \Psi_i}{\partial n_j} &= n_j \cdot \nabla \Psi_i = \text{Re} \left\{ -ju_j \left(\frac{dw_i}{dz_j} \right)^{**} \right\} \\ &= \text{Im} \left(u_j \frac{dw_i}{dz_j} \right) \end{aligned} \quad (27)$$

$$\text{and } u_j \frac{dw_i}{dz_j} = \frac{u_j}{u_i} \ln \frac{\hat{z}_j - z_{i+1}}{\hat{z}_j - z_i} \quad (28)$$

Now all the quantities of eqn. 11 are evaluated. As a word of caution, $\partial \Psi_i / \partial n_i$ is discontinuous at ΔC_i , equal to π internal to C , and equal to $-\pi$ external to C .

These formulas are easily programmed using either a complex algorithm or a real algorithm. We have written programs for both cases. An outline of a solution in terms of a piecewise-linear equivalent source is discussed in Appendix 8.2. The computer programs STEPSOURCE and LINEARSOURCE for the step-source solution and the piecewise-linear-source solution have been deposited in the IEE Program Library.

4 Test problems

Problems to test the accuracy and rate of convergence of the solution are easily constructed by choosing arbitrary

known solutions and arbitrary boundary shapes. The case $\Phi = 1$ on C was tried for several shapes, and typically gave $\Phi = 1$ in R to within 0.25% or better. The case when C is a circle of unit radius is interesting, because it illustrates the effect of k on the solution. If $k = 1$ and σ is a constant in eqn. 3, $\Phi = 0$ at the centre of the circle, regardless of the magnitude of σ . The problem becomes mathematically indeterminate, and requires infinite σ to produce a finite Φ . This cannot occur if we choose k according to eqn. 4. Physically, we can think of this restriction as requiring that positive σ produce positive Φ at every point on C . The matrix then becomes diagonally dominant, ensuring nonsingularity. Most computations were made with $k = 100$ and C bounded by the square $|x| = 1$ and $|y| = 1$.

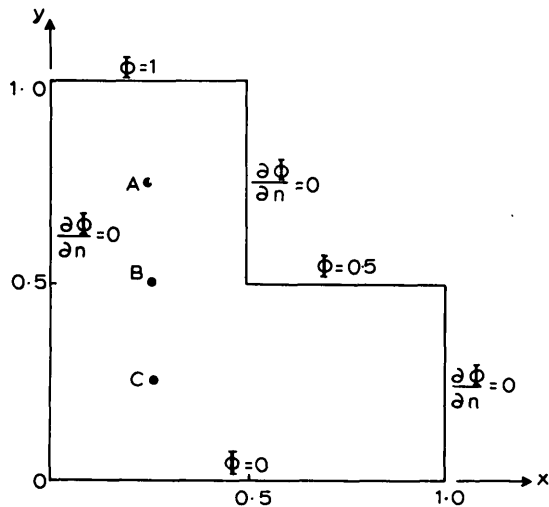


Fig. 3
Test problem to illustrate convergence

A second test problem is shown in Fig. 3. This is constructed by assuming that

$$\Phi = y \quad \text{in } R \quad (29)$$

and evaluating the boundary conditions on C as shown. To illustrate convergence, the problem was solved using eight segments ΔC_i , then 16, then 24 etc. The potential and its gradient were evaluated at the points A, B and C as shown. The approximate solution using pulse functions is compared to the exact solution in Table 1.

Table 1
POTENTIALS AND GRADIENTS COMPUTED FOR THE PROBLEM OF FIG. 3 USING N SEGMENTS

N	Φ_a	$ \nabla\Phi_a $	Φ_b	$ \nabla\Phi_b $	Φ_c	$ \nabla\Phi_c $
8	0.7360	0.9118	0.5060	0.9574	0.2614	0.9938
16	0.7482	0.9943	0.5012	0.9911	0.2519	1.0027
24	0.7491	0.9967	0.5004	0.9963	0.2508	1.0006
32	0.7495	0.9978	0.5002	0.9980	0.2504	1.0001
40	0.7497	0.9985	0.5001	0.9988	0.2502	1.0000
48	0.7498	0.9990	0.5001	0.9992	0.2502	1.0000
Exact	0.7500	1.0000	0.5000	1.0000	0.2500	1.0000

Additional test problems are easily constructed, and we have tried the programs on a number of them. Some general trends observed were:

- Specification of Φ on C tends to give more accurate solutions than specification of $\partial\Phi/\partial n$ on C . This is to be expected, because the original integral equation becomes more singular in the latter case.
 - Approximate solutions are more accurate in R away from C than on C . This is reasonable, because the effect of the approximation to σ becomes smaller the further we are from C .
 - The effect of k on the accuracy of the solution is very small,
- PROC. IEE, Vol. 116, No. 10, OCTOBER 1969

provided eqn. 4 is satisfied. Except when C was a circle, we obtained accurate solutions regardless of the choice of k .

5 Some applications

The computer programs can be used to calculate the Laplacian field inside or outside C , subject to arbitrary boundary conditions on C . Such problems arise in many diverse fields of physics, e.g. heat flow, fluid flow, electrostatics, magnetostatics etc. In this Section, we consider three types of electrical problems.

5.1 Resistance

The problem is to calculate the resistance between two conducting surfaces on or within a homogeneous conducting medium. If the thickness of the conductor is uniform, the problem is 2-dimensional. Fig. 4a shows the basic configuration. Conductor C_1 is maintained at a potential V_1 and conductor C_2 at a potential V_2 . The boundary condition over the rest of C is $\partial\Phi/\partial n = 0$. The electric-current flux is given by

$$J = gE = -g\nabla\Phi \quad (30)$$

where g is the conductivity of the medium. In complex notation, $\Delta\Phi$ is given by eqn. 25, and hence

$$\nabla\Phi = \sum_i \sigma_i \left(\frac{dw_i}{dz} \right)^* \quad (31)$$

$$\text{where } \frac{dw_i}{dz} = \frac{1}{u_i} \ln \frac{z - z_{i+1}}{z - z_i} \quad (32)$$

The notation of eqn. 31 means that $\text{Re}(\nabla\Phi) = \partial\Phi/\partial x$ and $\text{Im}(\nabla\Phi) = \partial\Phi/\partial y$, which are the x and y components of $\nabla\Phi$, respectively. The total current out of C_1 is

$$I = - \int_{C_1} J_n dc = g \int_{C_1} \frac{\partial\Phi}{\partial n} dc \quad (33)$$

This can be evaluated numerically by summing over the ΔC_j which belong to C_1 . The resistance between C_1 and C_2 is then

$$R = \frac{V_1 - V_2}{I} \quad (34)$$

Extension to a resistance system of M conductors C_1, C_2, \dots, C_M is straightforward.

5.2 Capacitance

A 2-body capacitance problem is illustrated by Fig. 4b. Here C_1 and C_2 are conductors maintained at

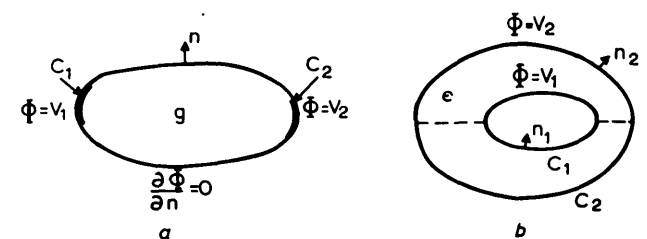


Fig. 4
Electrical properties
a Resistance
b Capacitance

potentials V_1 and V_2 , and the dielectric medium is homogeneous with permittivity ϵ . The electric-flux density is

$$D = \epsilon E = -\epsilon\nabla\Phi \quad (35)$$

where, in complex notation, $\nabla\Phi$ is given by eqn. 31. The charge per unit thickness on C_1 is

$$Q = -\epsilon \int_{C_1} D_n dc = \epsilon \int_{C_1} \frac{\partial\Phi}{\partial n} dc \quad (36)$$

which, again, can be evaluated numerically. The same charge

resides on the inside of C_2 , but there may be an additional charge on the outside of C_2 . The capacitance between C_1 and C_2 is

$$C = \frac{Q}{V_1 - V_2} \dots \dots \dots (37)$$

Extension to a multiconductor capacitance system is straightforward. Note the analogy between the resistance and the capacitance problems. Except for the boundary condition $\partial\Phi/\partial n = 0$ at a conductor boundary, the two problems are mathematically identical.

The available computer programs are written for a singly connected boundary, and require slight modifications to treat the multiply connected boundary of Fig. 4b. However, if the problem has one axis of symmetry, such as the broken line in Fig. 4b, the available computer programs can be applied to half of C_1 and C_2 connected by the broken line. The boundary condition on the broken line is $\partial\Phi/\partial n = 0$, as required by symmetry.

5.3 Transmission lines

The 2-conductor transmission-line problem is basically the same as the 2-conductor capacitance problem. If Fig. 4b represents the cross-section of a transmission line, the characteristic impedance is

$$Z_0 = \frac{\eta\epsilon}{C} \dots \dots \dots (38)$$

where $\eta = \sqrt{(\mu/\epsilon)}$ is the intrinsic impedance of the medium between the two conductors. If the conductors are perfect, the propagation constant is the intrinsic propagation constant of the medium. If the conductors are imperfect (e.g. they are metals), the attenuation constant is given by

$$\alpha_c = \frac{P_d}{2P_f} \dots \dots \dots (39)$$

Here P_d is the power dissipated per unit thickness in the conductors, and P_f is the power flow along the transmission line. The power dissipated in the walls is given by

$$P_d = r \int_{C_1+C_2} |H_c|^2 dc \dots \dots \dots (40)$$

where $r = \sqrt{(\omega\mu/2g_m)}$ is the surface resistance of the metal and

$$H_c = \frac{-1}{\eta} E_n = \frac{1}{\eta} \frac{\partial\Phi}{\partial n} \dots \dots \dots (41)$$

is the tangential component of magnetic field along C . The power flow along the transmission line is simply

$$P_f = \frac{|V_1 - V_2|^2}{Z_0} \dots \dots \dots (42)$$

where Z_0 is given by eqn. 38. Substitution from eqn. 40, via eqn. 42, into eqn. 39 gives

$$\alpha_c = \frac{Z_0 r}{2\eta^2 |V_1 - V_2|^2} \int_{C_1+C_2} \left| \frac{\partial\Phi}{\partial n} \right|^2 dc \dots \dots \dots (43)$$

which can be evaluated numerically once the boundary-value problem is solved. Again, the extension to a multiconductor transmission line is straightforward.

6 Discussion

The solution presented is easily applied to boundaries of an arbitrary shape and to arbitrary boundary conditions. The principal approximations are:

- (a) The contour is approximated by N straight-line segments.
- (b) The equivalent source is approximated as either a step function or a piecewise-linear function.
- (c) Boundary conditions are satisfied at discrete points on the boundary.

No further mathematical approximations are made. All these approximations can be carried to higher orders by general methods described in References 2 and 3. If the equivalent-source distribution is truly continuous, the piecewise-linear

solution converges faster than the step solution. However, for some boundary conditions and boundary shapes, the true equivalent-source distribution may be discontinuous. In this case, the step solution might be better than the piecewise-linear one.

The accuracy of the solution depends, in general, on the shape of the boundary and on the boundary conditions. For any particular problem, it depends on the number N of ΔC_i used. Since the solution involves a matrix inversion, we are restricted to N of the order of about 100, because of computing-time and storage considerations. If more accuracy than this is desired, more sophisticated analyses must be used.^{2,3} In the examples used to test the program, we never encountered any ill-conditioned matrices. A previous attempt by Cristal to solve the different integral eqn. 47 resulted in ill-conditioned matrices.⁶ Perhaps the reason for this is that eqn. 47 is a more singular equation than eqn. 3, which we used.

A quantitative comparison of our solution with the finite-difference method is given in Fig. 5. The finite-difference

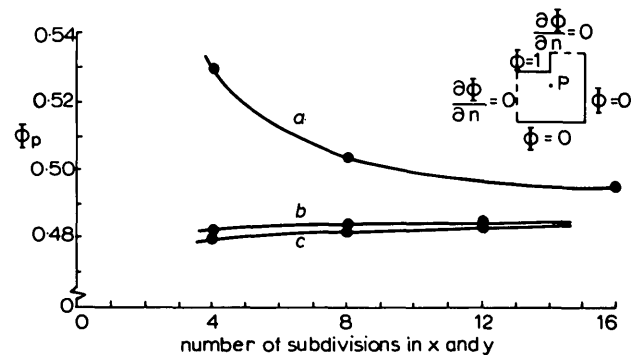


Fig. 5 Comparison of equivalent-source solutions and finite-difference solutions

- a Finite-difference solution
- b Piecewise-linear equivalent source
- c Step equivalent source

solution shown is that obtained by Schneider.⁷ The contour C and the boundary conditions are as shown in Fig. 5. The x -coordinate and the y -coordinate were each divided into equispaced increments, which defined the meshes in the finite-difference solution and the increments in the equivalent-source solution. A quantitative comparison with the finite-element solution⁸ has not been made.

Some qualitative comparisons of these methods are as follows. Both the finite-difference and finite-element solutions apply to a differential operator in the 2-dimensional space R . Our solutions apply to an integral operator on the 1-dimensional contour C . For given increments of length, better accuracy is to be expected from our solution, because integral operators are better behaved than differential operators. However, the finite-difference and finite-element solutions result in sparse matrices, and can be applied to larger matrices. The only fair comparison should be based on the time of computation required for a given accuracy.

A major advantage of our solution is the ease with which arbitrary boundary conditions can be treated. Treatment of boundary conditions by the usual finite-difference method is often complicated. Treatment of boundary conditions by the finite-element method is less complicated, but general boundary conditions of the type of eqn. 2 have not been considered.

The equivalent-source solution of this paper can be extended to regions which contain two or more homogeneous dielectrics. In this case, we need additional surface sources on the boundary contours dividing the dielectric regions. If the dielectrics are inhomogeneous, we must go to an integral over R , as discussed in the literature.³

We have used our solution with automatic-plot routines to give equipotential and gradient plots. The increments used for such plots can be as small as is desired, since the solution varies continuously in R . This is in contrast to the finite-difference solution, which is defined only at points in R , and to the finite-element solution, which is piecewise-linear in R . There may, of course, be some irregularities in

our solution on the boundary C due to the approximation to σ , but this effect is not noticeable at points in R away from C.

7 References

- 1 TRICOMI, F. G.: 'Integral equations' (Interscience, 1957)
- 2 HARRINGTON, R. F.: 'Matrix methods for field problems', *Proc. Inst. Elect. Electron. Engrs.*, 1967, 55, pp. 136-149
- 3 HARRINGTON, R. F.: 'Field computation by moment methods' (Macmillan, 1968)
- 4 HARRINGTON, R. F.: 'Time-harmonic electromagnetic fields' (McGraw-Hill, 1961)
- 5 WEBER, E.: 'Electromagnetic theory' (Dover 1965), chap. 7
- 6 CRISTAL, E. G.: 'Coupled rods between ground planes', *IEEE Trans.*, 1964, MTT-12, pp. 428-439
- 7 SCHNEIDER, M. V.: 'Computation of impedance and attenuation of TEM lines by finite difference methods', *ibid.*, 1965, MTT-13, pp. 793-800
- 8 ZIENKIEWICZ, O. C., and CHEUNG, Y. K.: 'The finite-element method in continuous structural mechanics' (McGraw-Hill, 1967)

8 Appendix

8.1 Integral equations

The usual derivation of integral equations from Laplace's equation involves the application of Green's theorem

$$\int \int_R (\Phi \nabla^2 \Psi' - \Psi' \nabla^2 \Phi) d\tau = \oint_C \left(\Phi \frac{\partial \Psi'}{\partial n} - \Psi' \frac{\partial \Phi}{\partial n} \right) dc \quad (44)$$

to the unknown field Φ and to the Green's function

$$\Psi(\rho, \rho') = \frac{1}{2\pi} \ln \frac{k}{|\rho - \rho'|} \quad (45)$$

The Green's function is the potential of a point source, i.e. the solution to

$$-\nabla^2 \Psi' = \delta(\rho - \rho') \quad (46)$$

where δ is the Dirac delta. Use of eqns. 45 and 46 in eqn 44 gives the familiar identity

$$\oint_C \left(\Phi \frac{\partial \Psi'}{\partial n} - \Psi' \frac{\partial \Phi}{\partial n} \right) dc' = \begin{cases} \Phi(\rho) & \rho \text{ in } R \\ 0 & \rho \text{ in } R' \end{cases} \quad (47)$$

where R is the region internal to C and R' is the region external to C. If eqn. 47 is applied to the surface just inside C, we obtain an integral equation. Note that both Φ and $\partial\Phi/\partial n$ are discontinuous across C in eqn. 47.

To derive the integral equation (eqn. 3), we apply eqn. 47 twice, once for the region R and once for R'. Letting superscript *i* denote quantities in R (internal to C) and *e* quantities in R' (external to C), we have

$$\left. \begin{aligned} \oint_C \left(\Phi^i \frac{\partial \Psi'}{\partial n} - \Psi' \frac{\partial \Phi^i}{\partial n} \right) dc' &= \begin{cases} \Phi^i & \rho \text{ in } R \\ 0 & \rho \text{ in } R' \end{cases} \\ -\oint_C \left(\Phi^e \frac{\partial \Psi'}{\partial n} - \Psi' \frac{\partial \Phi^e}{\partial n} \right) dc' &= \begin{cases} 0 & \rho \text{ in } R \\ \Phi^e & \rho \text{ in } R' \end{cases} \end{aligned} \right\} \quad (48)$$

The minus sign in front of the second equation arises from the direction of *n*, which is kept fixed. Now add eqns. 48 to obtain

$$\oint_C \left\{ (\Phi^i - \Phi^e) \frac{\partial \Psi'}{\partial n} - \left(\frac{\partial \Phi^i}{\partial n} - \frac{\partial \Phi^e}{\partial n} \right) \Psi' \right\} dc' = \Phi \quad (49)$$

where $\Phi = \Phi^i$ in R and $\Phi = \Phi^e$ in R'. An infinite number of integral equations is generated by choosing various Φ^e in R'. The least-singular integral equation is obtained by choosing $\Phi^i = \Phi^e$ on C, in which case eqn. 49 becomes

$$\oint_C \left(\frac{\partial \Phi^e}{\partial n} - \frac{\partial \Phi^i}{\partial n} \right) \Psi' dc' = \Phi \quad (50)$$

Eqn. 3 of the text is eqn. 50 with

$$\sigma(c') = \frac{1}{2\pi} \left(\frac{\partial \Phi^e}{\partial n} - \frac{\partial \Phi^i}{\partial n} \right) \quad (51)$$

The quantity $2\pi\epsilon\sigma$ can be thought of as the equivalent charge density on C which produces an electric potential Φ .

8.2 Piecewise-linear source solution

For a piecewise-linear approximation to σ , we use triangle functions³ $T_i(c)$, each extending over two adjacent ΔC , as shown in Fig. 6. Then, instead of eqn. 7, we have

$$\sigma \approx \sum_{i=1}^N \sigma_i T_i(c) \quad (52)$$

Eqn. 8 is still valid, except that

$$\Psi'_i(\rho) = \int_C T_i(c') \ln \frac{k}{|\rho - \rho'|} dc' \quad (53)$$

instead of eqn. 9. The midpoints of the triangle functions are at ρ_i , which are also the points of intersection of the

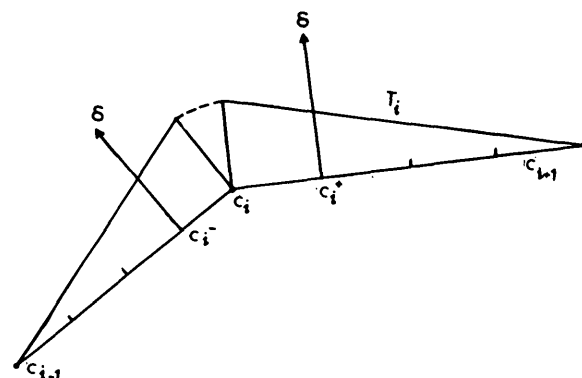


Fig. 6 Triangle function and Dirac-delta functions on contour C

ΔC . The normal direction at such points is discontinuous, and the normal derivative may be infinite there. Hence we cannot point-match at ρ_i . We could continue to point-match at the midpoints of the ΔC_i , but this can lead to singular matrices in some cases. (For example, Dirichlet boundary conditions on a square of side ΔC , point-matched at the centre of each side, gives rise to a singular matrix). To avoid such a possibility, define points which are one quarter of an interval on each side of ρ_i , and Dirac-delta functions at each point, as shown in Fig. 6. Define testing functions

$$t_i(c) = \delta(c - c_i^-) + \delta(c - c_i^+) \quad (54)$$

and the inner product

$$\langle f_1, f_2 \rangle = \oint_C f_1(c) f_2(c) dc \quad (55)$$

and apply the method of moments² to eqn. 5. The result is an

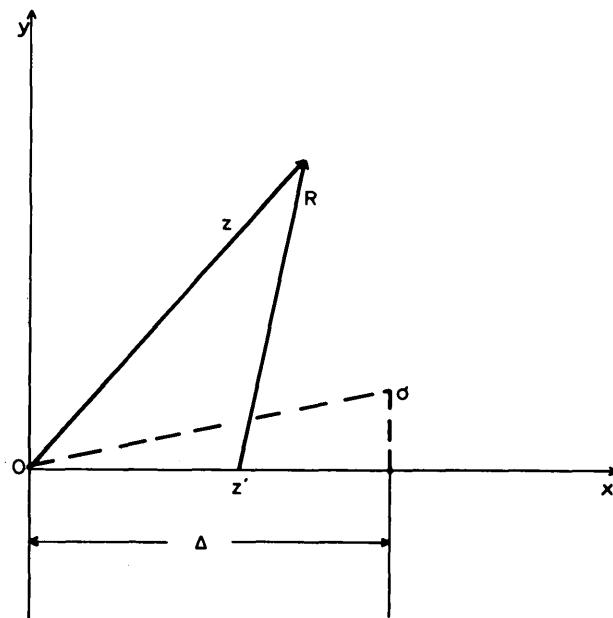


Fig. 7 Ramp source σ on an element Δ

equation of the form of eqn. 12, where the elements of $[l]$ and $[\gamma]$ are

$$l_{ji} = \langle t_j, LT_i \rangle \quad \dots \quad (56)$$

$$\gamma_j = \langle t_j, \gamma \rangle = \gamma(c_j^-) + \gamma(c_j^+) \quad \dots \quad (57)$$

In eqn. 56, L is the left-hand side of eqn. 12. Once $[l]$ is evaluated, equations of the type of eqns. 13–15 again apply.

To evaluate the l_{ji} , we need the potential and its gradient from triangle functions on C . Each triangle function is the sum of two ramp functions. Hence the basic source is a ramp function on each increment Δ . We can use complex-function theory, in the manner of Section 3, to evaluate the desired fields. Let Fig. 7 represent a ramp source σ on Δ , with local co-ordinates $z = x + jy$. Then the complex potential is

$$w = \frac{1}{\Delta} \int_{\Delta} z' \ln \frac{k}{z - z'} dz' \quad \dots \quad (58)$$

and the real potential is

$$\Psi = \text{Re}(w) = \frac{1}{\Delta} \int_{\Delta} x' \ln \frac{k}{R} dx' \quad \dots \quad (59)$$

These integrals are readily evaluated by integrating once by parts, and using the antiderivative of the logarithm. The result is

$$w = \frac{\Delta}{2} \ln \frac{k}{\Delta - z} + \frac{\Delta}{4} + \frac{z}{2} + \frac{z^2}{2\Delta} \ln \frac{z - \Delta}{z} \quad \dots \quad (60)$$

with Ψ given by eqn. 59. The gradient of the potential, in complex form, is given by eqn. 25. Differentiating eqn. 60, we obtain

$$\frac{dw}{dz} = 1 + \frac{z}{\Delta} \ln \frac{z - \Delta}{z} \quad \dots \quad (61)$$

The normal derivative at a point \hat{z}_j is again given by eqn. 27. The matrix elements l_{ji} are obtained by translating these results to global co-ordinates and evaluating eqn. 56. We shall not discuss the details; the results are given in the computer program LINEARSOURCE which has been deposited in the IEE Computer Program Library.

Discussion on

Divided-winding-rotor synchronous generator. A comparison of simulated 30MW conventional- and divided-winding-rotor turbogenerators and Improvement of alternator stability by controlled quadrature excitation

H. B. Laine: Both these papers are important contributions to our knowledge of the factors which influence the performance of alternating-current generators associated with large interconnected power systems.

The papers offer different approaches to the problems of absorption of reactive power and generator stability. Each discusses the use of unconventional windings on the rotor, in one case a divided winding with an effective angle of 60° between the two parts, and, in the other, a separate quadrature winding in addition to the conventional direct-axis-excitation winding. Each seeks to demonstrate significant improvements in reactive-power absorption in the range of stable operation, and tests theory by experiment on micromachines in one case, and in the other by the use of the mathematical model of Shackshaft [*Proc. IEE*, 1963, **110**, (4), pp. 703–713], together with experiments on a 5kVA motor-generator.

The papers are, and were intended to be, complementary to each other. I think that the underlying philosophy of both papers is in competition with that of high-speed voltage regulators acting on the direct-axis excitation of a conventional generator.

The problems of the absorption of reactive power and generator stability in large interconnected systems have been with us for a long time. 35 years ago it was a regular practice to switch out 66kV and 132kV cable circuits in the London area at times of light load, to keep the voltage below what was then thought to be the maximum permissible safe levels. Excursions into the zone of leading-power-factor operation of generating plant were regarded in most quarters as adventurous and hazardous, and generator instability a calamity to be avoided at all costs.

Paper 5773 P pays particular attention to an analysis of many arrangements of control feedback loops, and it comes to the conclusion, substantiated by practical results, that straightforward generator-angle feedback to the quadrature winding is adequate for the control of generators with load and reactive-power conditions which would be impossible to control by conventional means.

I thought the maximum reactive absorption was about -1.8 p.u., and this would appear to be accompanied by a fall in terminal voltage of more than 50%; but the simulation of a 30MW machine described in Paper 5680 P suggests that the generator terminal voltage was 1.1 p.u. (or just above) in the steady state condition, that a reactive absorption of -2.3 p.u. was obtained, and that this was not the limit of control. I would like to ask the authors where the limit of control actually lies, what the limiting parameter is, and to what extent it is dependent on the generator terminal voltage?

I note that there is a different approach in the two papers to the definition of the problem, in so far as Paper 5773 P appears to lump the transformer and line reactance together, whereas Paper 5680 P splits these quantities and the generator reactance into their various components.

Another interesting difference between the two approaches to the problem concerns the saliency which is related to the quadrature-axis reactance. The simulation in the case of the cylindrical-rotor 30MW turbogenerator used a saliency of 15% as stated in Section 5.1, whereas the Imperial College micromachine was a salient-pole alternator with about 22% saliency. Steady-state quadrature-winding generator-angle control is shown to operate satisfactorily on a salient-pole generator, as well as on a turbogenerator. Are the limits likely to be the same?

Is the basic reason for the claim that the transient stability of a machine with a divided-winding rotor is better than that of a conventional machine because it is not the axis of the rotor body which moves in relation to the axis of the rotating field in the stator, but rather the axis of the resultant m.m.f. provided in the rotor by the two windings?

I should like to know the difference between a phasor diagram and what I would have called a vector diagram. Is there a good reason for this difference in description?

It would be of real advantage to the economic operation of a large interconnected power system, such as that of the Generating Boards, if the reactive-power requirements, both positive and negative, could be met at all times by the most economic generating plant which the load demands, with a minimum use of shunt reactors or synchronous compensators.

V. Easton: I was present in 1965 at a demonstration

Paper 5680 P by SOPER, J. A., and FAGG, A. R. [see **116**, (1), pp. 113–126] and Paper 5773 P by KAPOOR, S. C., KALSI, S. S., and ADKINS, B. [*Proc. IEE*, 1969, **116**, (5), pp. 771–780]
Read before the IEE Power Division, Professional Group P1, 31st April 1969